25th European Photovoltaic Solar Energy Conference,
6-10 September 2010, Valencia, Spain, 3078 - 3082

SURFACE CHARACTERIZATION OF SPUTTERED ZNO:AL FOR SILICON THIN-FILM SOLAR CELLS

G. Jost*, E. Bunte, J. Worbs, H. Siekmann, J. Hüpkes
IEF-5 Photovoltaik, Forschungszentrum Jülich GmbH, 52425 Jülich, Germany
*phone: +49 2461 61 6310, fax: +49 2461 61 3735, email: g.jost@fz-juelich.de

ABSTRACT: Using a large range of differently deposited ZnO:Al substrates we investigated the correlation between the as-deposited ZnO:Al surface and the resulting surface topography of ZnO:Al after texture-etching in diluted hydrochloric acid. SEM images of the unetched surface were employed to characterize different features of the unetched topography. Based on these findings a new surface classification is suggested. SEM results show that ZnO:Al samples with similar features before etching also show strong resemblance in their surface topography after etching. Furthermore we prove that certain features of the unetched surface are optically measurable via haze measurements and can therefore be used to predict the etch results. Angular resolved scattering measurement and SEM images of the etched surface are used to evaluate the results of the etching step. Finally, µc-Si solar cells are assembled on the ZnO:Al films. We show that the short circuit current density of the test cells is correlated to the angular resolved scattering signal of discrete large angles.
Keywords: ZnO:Al, surface topography, light-scattering

1 INTRODUCTION

ZnO has been attracting a lot of attention as new transparent conductive oxide in superstrate configurations of silicon based thin-film solar cells [1]. Due to its good durability against hydrogen plasma [2] it is generally applied as front contact and therefore optimized with respect to transparency, conductivity and light-scattering behavior.
There are various methods to deposit highly transparent and conductive ZnO thin-films which include amongst others, low pressure chemical vapor deposition (LPCVD), metal organic chemical vapor deposition (MOCVD) and sputter deposition [3, 4, 5]. The most common method for large area ZnO:Al deposition is the sputter technique which is also subject of this paper.

Previous studies have demonstrated that not only the transparency but also a well-textured TCO surface at the silicon interface is relevant for a good solar cell conversion efficiency as it facilitates light-scattering and thus light-trapping in the solar cell [6, 7]. As sputtered ZnO:Al typically does not feature a significant roughness after deposition, it has to be textured in an additional process to yield adequate light-scattering properties. A method for texturing that is often applied is a wet-chemical etching step in diluted hydrochloric acid (0.5% HCl). However, even under constant etching conditions the results of the texture-etching vary depending on the film properties which are subject to the deposition parameters [8, 9].

As the cell performance rises and falls with the texture etch result, it is inevitable to develop a process control to ensure industrial applicability of ZnO:Al as front contact in thin-film silicon solar cells. Various publications have already addressed means for characterizing ZnO:Al surfaces with different topography via atomic force microscopy analysis or angular resolved scattering measurements [10, 11, 12]. However, they still lack the answer of how much certain surface topographies influence the cell performance. Additionally, prediction of etching morphology from the as-deposited state is difficult but in [13] a relationship between as-deposited ZnO:Al surface characteristics and the etch results is indicated.

In this paper we will present a variety of differently sputtered ZnO:Al thin-films. We will show that deposition-dependent differences in ZnO:Al thin-films can already be determined on the surface of the unetched films and thus the outcome of the etching step can be predicted from film properties rather than from deposition conditions. Furthermore we will also demonstrate that additional optical measurements of the texture-etched ZnO:Al enable a prediction of the expectable short circuit current density of µc-Si solar cells on the investigated ZnO:Al.

2 EXPERIMENTAL

2.1 Sample Preparation

All ZnO:Al thin-films discussed in this paper were deposited on Corning Eagle 2000 substrates in an in-line sputter system (VISS 300 by VAAT). The sputter system was operated at radio frequency mode (RF). The target in use was a 750 mm x 100 mm planar ceramic target $ZnO:Al_2O_3$ (99:1 wt%). As inert gas for plasma generation Argon (Ar) was utilized. All films were deposited in a dynamic mode with a carrier passing the targets several times. Thus an in-line production with multiple targets is simulated. The deposition parameters were varied to facilitate the growth of numerous ZnO:Al thin-films with different properties. Amongst the altered deposition parameters were substrate temperature, process pressure, Argon gas-flow, an additional Ar/O_2-gas intermixture and the applied discharge power. The interval for all varied process parameters is displayed in Table I. To ensure a similar film thickness of ca. 750 nm for all samples the number of passings and the carrier speed was adjusted accordingly. All samples were texture-etched in a 0.5% HCl dissolution with adjusted etching times to compensate for different etch rates thus leading to a removal of ca. 150 nm for each sample. All wet-chemical etching was conducted at room temperature. The texture-etched samples were applied as front-contacts in µc-Si thin-film solar cells with a total thickness of 1.2 µm of the pin-structure, an 80 nm thick ZnO:Al back contact and a silver reflector of ca. 0.7 µm thickness. Further details on sample preparation is described elsewhere [14, 15].

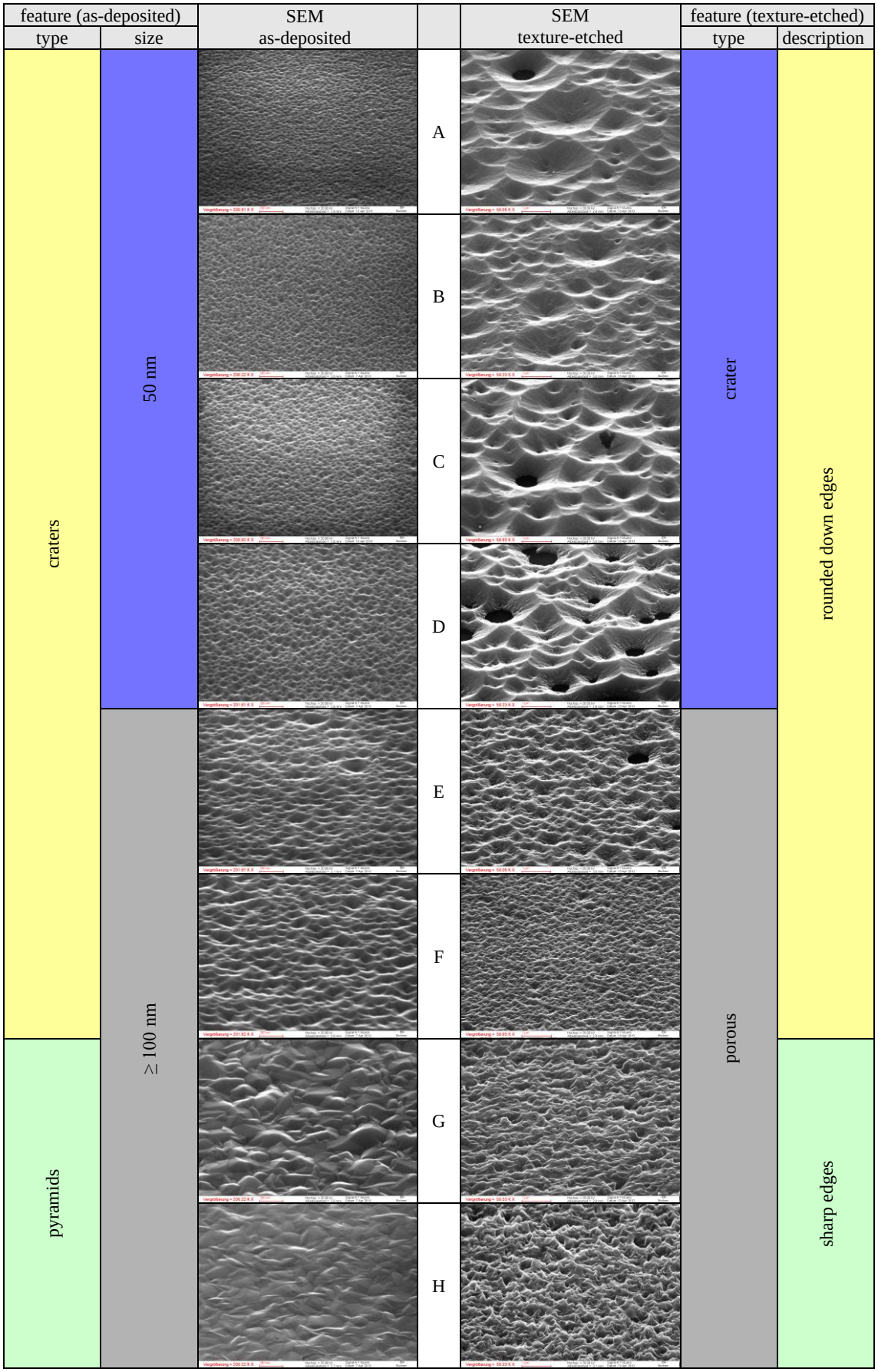

Figure 1: SEM images of ZnO:Al surface before and after texture etching in 0.5% HCl

Table I: interval of process parameters

deposition parameter	min	max
power (kW)	1	2
Ar flow (sccm)	35	65
O_2 portion (‰)	0	0.3
pressure (µbar)	0.7	5
temperature (heater) (°C)	170	470

2.2 Sample characterization

All samples were characterized at different states of their preparation. The first sample characterization was performed directly after the ZnO:Al film deposition. The yet unetched samples were characterized with optical measurements including measurements of total and diffuse transmission as well as reflectance for a wavelength interval of 300 nm to 1300 nm with a double beam spectrometer (Perkin Elmer Lambda 19). Additionally high resolution SEM images of the ZnO:Al surface were taken to evaluate the surface topography. The same measurements were repeated after the texture-etch step in 0.5% HCl. Additionally in this production stage angular resolved scattering (ARS) measurements were conducted under illumination of a laser with a wavelength of 550 nm to reveal the angular distribution of scattered light. In the test set-up used the incident light-beam is perpendicular to the substrate surface. The exit angle of the light is measured in relation to the substrate normal. Thus exiting light at 0° is perpendicular to the substrate surface whereas scattered light at 90° is parallel to the substrate surface.
In a final step the completed µc-Si solar cells were tested and their I/V-characteristics measured for an illumination under AM 1.5 solar spectrum at 25°C and an additional filter (OG 590) in the optical path. Details on solar cell characterization are described elsewhere [16].

3 RESULTS AND DISCUSSION

3.1 SEM analysis before and after texture etching

Up to now not much attention was paid to the as-deposited surfaces of sputtered ZnO:Al. Using high resolution SEM of as-deposited ZnO:Al, distinct structures on the surface become visible (see left hand side of Fig. 1). These structures differ in shape and size. There are two primary shapes on as-deposited ZnO:Al that can be distinguished: crater type structures and pyramid type (or grain) structures. Crater type structures can be seen in Fig. 1 samples A through F (yellow) on the as-deposited SEM-images whereas pyramid type structures are visible for samples G through H (green). However, not only the feature shape underlies variations, but also the feature size. Samples A through D inhibit an average feature size of ca. 50 nm (blue) whereas samples E through G show a larger average size of about 100 nm and more (grey). Taking the etched surfaces (see right hand side of Fig. 1) into account a correlation between as-deposited texture and etched texture appears. All samples with feature size of about 50 nm as-deposited (A-D) develop a surface with distinct large craters whereas all samples with as-deposited average features sizes equal or larger than 100 nm (E-H) develop a porous surface that lacks large size craters. Thus the feature size of the as-deposited samples can be used to predict the topography after etching.

However, not only the feature size but also the feature type (crater, pyramid) of the as-deposited sample provide information on the etched topography. For samples with feature sizes ≥ 100 nm craters on the unetched surface (E-F) lead to a porous film with rounded edges when etched. Samples with pyramids on the as-deposited surface (G-H) on the other hand show porous films with sharp edges after the texturing step.

So far all etched ZnO:Al surfaces have been characterized into type I, II and III [17] where type I resembles samples E-H, type II sample C-D and type III sample A-B of the SEM-images presented in Fig. 1 (right). However, in accordance with the results of before and after etching SEM-image classification we propose a distinction between porous type and crater type.

3.2 Optical properties before etching - haze

As presented in section 3.1 sputtered ZnO:Al surfaces can be distinguished via SEM imaging. However, as SEM-imaging is a complex and expensive method other means for measuring the differences in ZnO:Al surfaces were investigated. Fig. 2 shows the spectral haze of the as-grown ZnO:Al films in Fig. 1. Half of the films (A-D) show a very low haze (<1%) for the entire spectral range measured. However, some of the films (E-H) show a distinct haze >1% for wavelengths below 450 nm. The light-scattering ability of the measured films correlates with the surface features size. The average feature size (~50 nm before etching) is too small to facilitate an optical haze greater than 1% in the visible range. This can be seen for samples A through D in figure 2. All samples that reveal a porous surface after etching exhibit such feature sizes of 100 nm or greater before etching that enable light-scattering for wavelengths in the visible range. Therefore these samples all show a haze greater than 1% (up to 5%) in the visible range as can be seen in figure 2 for samples E through H. The haze decreases with increasing wavelength of the incident light as the surface features become too small in relation to the wavelength and therefore cannot induce light-scattering anymore. Thus the haze of as-deposited samples proves to be a suitable measure for distinguishing between crater type and porous type even before etching.

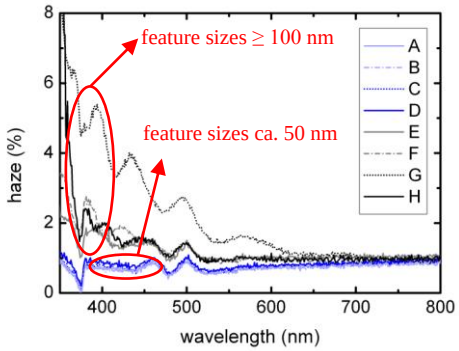

Figure 2: results of haze measurements of as-deposited ZnO:Al

3.3 Optical properties after etching – angular resolved scattering (ARS)

After etching the samples in 0.5% diluted HCl light-scattering becomes significant for all films and haze increases. For further analysis angular resolved scattering measurements were performed on the ZnO:Al surface.

The results for angles from 0° to 90° are plotted in figure 3. Again the set of samples divides clearly into the two groups: crater type and porous type. Samples with a crater type surface show a distinctly higher angular resolved light-scattering signal for angles from 0° to 30° than for the larger angles till 90°. This is demonstrated in figure 3 by samples A through D. Samples with a porous surface after etching show a significantly lower signal for angles from 0° to 30° which is comparable with the ARS signal of larger angles. This is illustrated in figure 3 by samples E through H.

That way also angular resolved light-scattering can be applied to measure the differences between porous and crater type surface and thus is a valuable measure to distinguish between the two topography types after texture-etching.

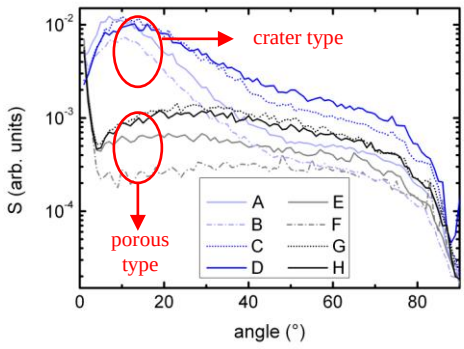

Figure 3: results of angular resolved scattering (ARS) measurements of texture-etched ZnO:Al

3.4 Cell results and correlation with previous characterization of ZnO:Al.

In section 3.3 angular resolved light-scattering was used to analyze the surface topography. Further analysis of the ARS signal for large angles (≥ 50°) of the texture etched ZnO:Al in relation to the short circuit density of the thereupon deposited µc-Si solar cells show a correlation between the two measuring values. In figure 4 the short circuit current density measured with red filtered light is plotted against the ARS signal of discrete angles (≥ 30°). With increasing ARS signal of large angles the short circuit current density increases. Note that the x-axis is in logarithmic scale.

The best results appear for 60° whereas 50° and 70° show more deviations from the almost logarithmic function at 60°. For angles smaller than 50° this correlation does not apply as can be seen in Fig. 4 for 30°. For angles greater than 70° the measured ARS-signal (not shown) is getting lower and lower approaching zero for 90° and therefore too sensitive to measurement errors.

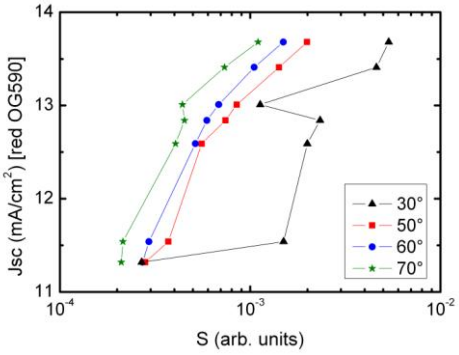

Figure 4: short circuit current density of various solar cells plotted against ARS results of discrete angles

4 CONCLUSION

In this study the predictability of texture etch results of sputtered ZnO:Al was investigated. A correlation between as-deposited surface topography and textured surface topography was found. A new classification of textured surfaces in two types – crater and porous – is suggested and it was proven that a differentiation before – via haze – and after etching – via ARS – is possible.

Additionally a correlation between the optical properties of a textured ZnO:Al front contact and the short circuit current density of a hereupon manufactured µc-Si solar cell was suggested by showing that an increasing ARS signal for large angles leads to an increasing short circuit current density of the solar cell. Thereby the short circuit current densities of µc-Si cells become a predictable property which presents the first step to process control for thin-film silicon solar cells on texture-etched ZnO:Al front contacts.

ACKNOWLEDGMENTS

The authors would like to thank B. Zwaygardt, J. Kirchhoff, A. Gordijn and H.P. Bochem for technical assistance and fruitful discussions. We gratefully acknowledge financial support by BMU (contract No. 0327693A)

REFERENCES

[1] J. Müller, G.Schöpe, O. Kluth, B. Rech, V.Sittinger, B. Szyszka, R. Geyer, P. Lechner, H. Schade, M. Ruske, G. Dittmar, H.P. Bochem, Thin Solid Films, 442 (2003) 158-162

[2] O. Kluth, B. Rech, L. Houben, S. Wieder, G. Schöpe, C. Beneking, H. Wagner, A. Löffl, H.W. Schock, Thin Solid Films, 351 (1999) 247-253

[3] I. Volintiru, M. Creatore, B.J. Kniknie, C.I.M.A. Spee, M.C.M. van de Sanden, Journal of Applied Physics, 102 043709 (2007)

[4] S. Fay, J. Steinhauser, N. Oliveira, E. Vallat-Sauvain, C. Ballif, Thin-Solid Films, 515 (2007) 8558

[5] J. Hüpkes, J. Müller and B. Rech, Transparent Conductive Zinc Oxide – Basics and Applications in Thin Film Solar Cells, ISBN 978-9-540-73611-0, p. 359-413

[6] M. Berginski, J. Hüpkes, W. Reetz, B. Rech, M. Wuttig, Thin Solid Films, 516 (2008) 5836-5841

[7] C. Beneking, B. Rech, S. Wieder, O. Kluth, H. Wagner, W. Frammelsberger, R. Geyer, P. Lechner, H. Rübel, H. Schade, Thin Solid Films, 351 (1999) 241-246
[8] J. Hüpkes, B. Rech, S. Calnan, O.Kluth, U. Zastrow, H. Siekmann, M. Wuttig, Thin Solid Films, 502 (2006) 286-291
[9] O. Kluth, G. Schöpe, J. Hüpkes, C. Agashe, J. Müller, B. Rech, Thin Solid Films, 442 (2003) 80-85
[10] O. Kluth, C. Zahren, H. Stiebig, B. Rech, H. Schade, Proc. 19th European Photovoltaik Solar Energy Conference, Paris, France, 2004
[11] A. Krasnov, Solar Energy Materials and Solar Cells (2010), doi: 10.1016/j.solmat.2010.05.022
[12] T. Repmann, W. Appenzeller, T. Roschek, B. Rech, H. Wagner, Proceedings of the 28th IEEE Photovoltaic Specialists Conference, Anchorage, 2000, p. 912-915
[13] H. Zhu, J. Hüpkes, E. Bunte, S.M. Huang, Surface and Coatings Technology (2010), doi: 10.1016/j.surfcoat.2010.07.122
[14] J. Hüpkes, H. Zhu, J. Owen, G. Jost, E. Bunte, Proceedings of the 8th Int. Conf. on Coatings on Glass and plastics, Braunschweig, 2010, p. 439-443
[15] W. Dewald, V. Sittinger, B. Syzszka, A. Gordjin, J.Hüpkes, F. Hamelmann, H. Stiebig, F. Säuberlich, Proceedings of the 8th Int. Conf. on Coatings on Glass and plastics, Braunschweig, 2010, p. 415-416
[16] W. Reetz, T. Kirchartz, A. Lambertz, J. Hüpkes, A. Gerber, Proceedings of the 24th EUPVSEC, Hamburg, p. 2784-2788 (2009)
[17] M. Berginski, J. Hüpkes, M. Schulte, G. Schöpe, H. Stiebig, B. Rech, M. Wuttig, Journal of Applied Physics 101, 073101 (2007)